Romenskyy, M., Herbert-Read, J. E., Ioannou, C. C., Szorkovszky, A., Ward, A. J. W., & Sumpter, D. J. T. (2019). Quantifying the structure and dynamics of fish shoals under predation threat in three dimensions. *Behavioral Ecology*, [arz197]. https://doi.org/10.1093/beheco/arz197

Peer reviewed version

Link to published version (if available):
10.1093/beheco/arz197

Link to publication record in Explore Bristol Research
PDF-document

This is the author accepted manuscript (AAM). The final published version (version of record) is available online via Oxford University Press at https://academic.oup.com/beheco/advance-article/doi/10.1093/beheco/arz197/5628877 . Please refer to any applicable terms of use of the publisher.

University of Bristol - Explore Bristol Research
General rights

This document is made available in accordance with publisher policies. Please cite only the published version using the reference above. Full terms of use are available:
http://www.bristol.ac.uk/red/research-policy/pure/user-guides/ebr-terms/

# Quantifying the structure and dynamics of fish shoals under predation threat in three-dimensions

Maksym Romenskyy*,[1] James E. Herbert-Read*,[2,3] Christos C. Ioannou,[4]
Alex Szorkovszky,[5] Ashley J. W. Ward,[6] and David J. T. Sumpter[5]

[1] *Department of Life Sciences, Faculty of Natural Sciences, Imperial College London, London SW7 2AZ, United Kingdom*
[2] *Department of Zoology, University of Cambridge, Cambridge, CB2 3EJ, United Kingdom*
[3] *Department of Biology, Aquatic Ecology Unit, Lund University, Lund, 22362, Sweden*
[4] *School of Biological Sciences, University of Bristol, Bristol, BS8 1TQ, United Kingdom*
[5] *Department of Mathematics, Uppsala University, Box 480, Uppsala 75106, Sweden*
[6] *School of Biological Sciences, University of Sydney, Sydney, New South Wales, Australia*

Detailed quantifications of how predators and their grouping prey interact in three dimensions (3D) remain rare. Here we record the structure and dynamics of fish shoals (*Pseudomugil signifer*) in 3D both with and without live predators (*Philypnodon grandiceps*) under controlled laboratory conditions. Shoals adopted two distinct types of shoal structure; 'sphere-like' geometries at depth, and flat 'carpet-like' structures at the water's surface, with shoals becoming more compact in both horizontal and vertical planes in the presence of a predator. The predators actively stalked and attacked the prey, with attacks being initiated when the shoals were not in their usual configurations. These attacks caused the shoals to break apart, but shoal reformation was rapid, and involved individuals adjusting their positions in both horizontal and vertical dimensions. Our analyses revealed that targeted prey were more isolated from other conspecifics, and were closer in terms of distance and direction to the predator compared to non-targeted prey. Moreover, which prey were targeted could largely be identified based on individuals' positions from a single plane. This highlights that previously proposed 2D theoretical models and their assumptions appear valid when considering how predators target groups in 3D. Our work provides experimental, and not just anecdotal, support for classic theoretical predictions, and also lends new insights into predatory-prey interactions in three-dimensional environments.

Keywords: group living, 3D, predation, collective behavior, *Pseudomugil signifer*

## INTRODUCTION

Moving animal groups, such as flocks of birds, shoals of fish, and swarms of arthropods form spectacular three-dimensional group structures while on the move together (Attanasi *et al.* 2014, Ballerini *et al.* 2008, Brierley & Cox 2010, Johnsen *et al.* 2017, Major & Dill 1978, O'Brien 1989, Parrish & Hamner 1997, Partridge *et al.* 1980, Ward & Webster 2016). Technologies such as stereo-imaging and high-resolution multi-beam sonar have allowed researchers to quantify the dynamic, large-scale structures of animal groups (Gerlotto & Paramo 2003, Guillard *et al.* 2011, Handegard *et al.* 2017, Paramo *et al.* 2010). While these technologies have highlighted the extraordinary range of structures groups can adopt, controlled and manipulative studies to assess how groups adapt their structure in response to both their position in space and to external perturbations are rare (Abrahams & Colgan 1985, Hemelrijk *et al.* 2010, Partridge *et al.* 1980, Viscido *et al.* 2004). Such studies are vital, however, if we are to understand the ecological and evolutionary drivers of collective behavior, and the costs and benefits of individuals adopting different positions in groups across all spatial dimensions that animals live (Krause 1994).

Predation is considered to be a primary driver shaping how individuals in groups interact (Ioannou *et al.* 2012; 2011, Seghers 1974), and some of the most spectacular examples of groups changing their structure occur when groups are under predatory attack (Axelsen *et al.* 2001, Carere *et al.* 2009, Magurran & Pitcher 1987, Pitcher & Wyche 1983). Our understanding of why animals adopt particular group configurations in response to threat stems from some early theoretical, and later empirical work on the subject. Hamilton (1971), for example, explained how gregarious behaviors could be selected for by individuals attempting to reduce their 'domains of danger' in the presence of a predator, causing them to move closer to near neighbors. Vine (1971) suggested that groups should form different three-dimensional structures depending on their location with respect to boundaries in the environment. In particular,

* – these authors contributed equally
Authors for correspondence: m.romenskyy@imperial.ac.uk; james.herbert.read@gmail.com

if individuals attempt to minimise their domains of danger from predators attacking from the outside of groups, then they should form flatter circular configurations at boundaries, whereas they should form spheroid structures in open space (Vine 1971). These ideas were later refined by incorporating biologically important constraints, such as limited movement and perceptual ranges of prey and predators (Chen & Kolokolnikov 2014, James *et al.* 2004, Morrell *et al.* 2010; 2011, Yang & Schmickl 2019).

Measurements from the field and under semi-natural conditions confirmed predictions that groups change their density, shape and structure, both in the presence or absence of predators, but also in direct response to attacks (Axelsen *et al.* 2001, Carere *et al.* 2009, Nøttestad *et al.* 2002, Pitcher & Wyche 1983, Procaccini *et al.* 2011, Rieucau *et al.* 2014; 2016). However, such observations have usually been limited to broad scale characterisations of the structure of groups, often in a single plane, without experimental evidence showing how groups change their structure depending on their location in space and in response to the movements of predators. With some notable exceptions of fine-scale measurements of predatory-prey interactions in the wild (Benoit-Bird & Au 2009, Handegard *et al.* 2012), it remains unclear how groups use space to move and self-organise when under threat from real predators in three-dimensions.

While measuring how animal groups adjust their density, shape and size in response to predatory attacks sheds light on the emergent properties that result from individuals adjusting their social interaction-rules (Couzin *et al.* 2002, Hemelrijk & Hildenbrandt 2012, Herbert-Read 2016), it is also important to consider the relative risk that individual prey face depending on their location within groups. When predators attack individual prey in groups, this risk will be related to the strategies that predators use when attempting to select targets from within the group. Previous empirical evidence shows that isolated individuals, or individuals on the edges of groups experience greater risk of predation (Duffield & Ioannou 2017, Ioannou *et al.* 2019, Krause *et al.* 2017), but these studies have also been limited to individuals' relative risk in a single plane. Further, most models investigating so-called 'marginal predation' have only considered this from a two-dimensional approach (Hamilton 1971, Hirsch & Morrell 2011, Viscido *et al.* 2001). For some systems, where prey form two-dimensional group structures, this approach is clearly warranted (De Vos & O'Riain 2010, Romey *et al.* 2007, Watts *et al.* 2017), but in systems where animals use both the vertical and horizontal planes to move, it is necessary to investigate whether the predictions, and assumptions of the models, hold true. Indeed, in Hamilton's original model, it was proposed that predators could attack from anywhere within the group, but this assumption that was later critiqued, with it being suggested that predators may only attack from the outside of groups (Vine 1971, Viscido *et al.* 2001).

In this paper, we investigate the spatio-temporal dynamics of shoals of Pacific blue-eyes (*Pseudomugil signifer*) in three dimensions in the presence and absence of a sympatric predator, flat-headed gudgeon (*Philypnodon grandiceps*). We first asked whether the presence of a predator changes the three-dimensional spatial properties of shoals. We predicted, according to theory, that the area of the shoals in both vertical and horizontal planes should become smaller following introduction of the predator as individuals attempt to minimise their (limited) domains of danger (Hamilton 1971, James *et al.* 2004). We also predicted that individuals should adopt distinct 3D structures depending on their location with respect to boundaries in their environment (Vine 1971). We next investigate the complete sequence of behavioral states characterising the predator-prey dynamics, and assessed the key dynamical properties of the shoals on a fine-resolution scale before, during and after an attack. Finally, we ask what factors increase the likelihood that a prey will be targeted by the predator in 3D, predicting that more isolated individuals should be at greater risk, and asked whether information from both horizontal and vertical planes were needed to predict this risk.

## MATERIALS AND METHODS

### Animal husbandry and housing

Pacific blue-eyes (*Pseudomugil signifer*) (18.2 ± 2.4 mm; mean ± SD) and flat-headed gudgeon (*Philypnodon grandiceps*) (50.8 ± 4.5mm; mean ± SD) were caught with hand nets from Narrabeen Lagoon, New South Wales, Australia (33°43'03" S, 151°16'17" E). These species are sympatric, and flat-headed gudgeon naturally prey on small fish species (Becker & Laurenson 2008, Pusey *et al.* 2004), such as Pacific blue-eyes. The two species were housed separately in filtered freshwater in 150 l tanks at 22 - 25 °C in the laboratory. Pacific blue-eyes were housed in groups of $< 140$ individuals per tank. Pacific blue-eyes were moved between different tanks to keep used and un-used fish separated (see below). Tanks contained artificial plants, gravel and shelters (semi-circular plastic tubes). Fish were held on a 12:12 light:dark cycle. All fish were housed for at least two weeks prior to experimentation. Pacific blue-eyes were fed five times per week on crushed flake food *ad libitum*, and flat-headed gudgeon on 2 mm sinking pellets *ad libitum*. On the day of trials, fish were fed after experimentation.

### Data acquisition

The experiment consisted of filming and recording the behavior of Pacific blue-eyes in the absence and presence of a flat-headed gudgeon in an experimental arena. The experimental arena (see Figure S1) was a glass aquarium (420×275×365 mm length x width x height) filled to a depth of 315 mm with aged and conditioned tap water which was aerated between each day of trials using an air-stone. We did not change water between trials, although the water level was topped-up with fresh water between days. We used opaque white plastic (5 mm thickness) to cover the bottom and three sides of the arena. The plastic on the back wall was angled in order to avoid blind spots in the camera's field of view. The arena was lit by fluorescent lamps placed horizontally on either side of the experimental tank. The two orthogonal projections of the experimental arena (horizontal, XY-plane and vertical, XZ-plane) were filmed by a single camera. The vertical plane was captured by a camera positioned orthogonally to that plane and the horizontal plane was captured by the same camera through a mirror angled at $\sim 45°$ and placed above the arena. The use of a slanted mirror enabled a simple reconstruction of the Y-coordinates from the XY projections onto the mirror (Chrásková *et al.* 1999). We used a Nikon D7000 DSLR camera with the centre of its objective lens (Nikon AF-S DX Nikkor 35mm f/1.8G) positioned at height of 315 mm, equivalent to the water's surface, to record the trials at 24 fps at a resolution of 1920×1080 pixels. The videos were recorded in .mov format using H.264 camera compression.

### Camera calibration and animal tracking

Before filming began on each day, we first performed geometric camera calibration. In the first calibration step, we placed a calibration board (5×4 black-and-white checkerboard, square size 32×32 mm) under water in the arena in an orientation in which the calibration pattern was visible in both filming planes (see Figure S2 for an example of the calibration images). We then took a snapshot of the scene and repeated this procedure for 13-16 different configurations of the board in the aquarium. The camera did not move during and after this calibration step. The next calibration step was performed after filming. During this step, the correspondences between the elements of the calibration pattern in two camera views were used to reconstruct the three-dimensional real-world position of the camera with respect to the scene and to obtain camera calibration matrices. This step was performed in MATLAB following standard calibration procedures (Hartley & Zisserman 2003). The calibration matrices were then applied to tracking data to reconstruct the 3D positions of individual fish and positions of fish shoals.

We used different approaches to record the positions of the prey and predator. We used Didson Tracking Software (Handegard & Williams 2008) to track the positions of the prey in both the side view of the camera, and the view in the mirror. We used CTrax software (Branson *et al.* 2009) to record the trajectory of the predator. Because of the unavoidable internal reflections caused by the side of glass that had not been covered with white plastic (in the mirror plane), we removed a small segment from the arena where this occurred as tracking proved difficult in this region. In all other areas, the position of the predator was manually corrected with the Matlab GUI, fixerrors, associated with the CTrax software. This way we could get reliable positions and orientations of the predator in both planes.

### Experimental protocol

For each trial, we randomly selected 15 Pacific blue-eyes of similar size and transferred them into the experimental arena. Fish were left to acclimate to the arena for at least 5 minutes, after which the filming commenced. Fish were filmed in the arena for 20 minutes before we introduced a flat-headed gudgeon. Apart from during times when the predator was being added to the arena, fish did not have a line of sight to the experimenter. Interactions between the predator and prey were recorded for a further 60 minutes for each trial, giving a total of 80 minutes of video for every replicate (n = 16). This equated to 320 minutes of footage of prey without the predator, and 960 minutes of footage of predator with the prey. In total we used four different predators. Each predator was only used only once per day, and each predator was only used four times in total. Predators that had and had not been used on a single day were kept in two separate housing tanks. Because we did not house each predator separately, we could not include predator identity in our analyses. Pacific blue-eyes were not used more than once and used fish were housed separately from non-experimented fish. Two to four trials were performed each day, with five days of testing in total. There was a maximum of three days between consecutive days of testing (a minimum of one). All trials were run between 0900 - 1700 hrs.

## Data Processing and Statistical Analysis

All motion and statistical analyses were performed using custom scripts in MATLAB R2016b, R, and Python 2.7.

### *Assessing the structure of the fish shoals*

From the prey's coordinates, we calculated the shoal's projected area in both horizontal and vertical planes for each frame of the video. The vertical plane consisted of data from fish's positions in the XZ plane (and not the YZ plane), although we note that for this vertical dimension, these labels are largely arbitrary (see Figure S1). To measure the area of a shoal in each planar projection (XY or XZ), we first constructed the tightest fitting alpha shape which enclosed all fish's coordinates without spitting the shoal into several subgroups. We therefore defined the alpha shape as a boundary that envelops coordinates of all prey in a given frame and computed it using the MATLAB inbuilt `AlphaShape` function. The area of the resulting alpha shape was then computed with the standard MATLAB function `Area`.

We used a model comparison approach to assess what factors best predicted the shoal's area. Linear mixed effects models (LMMs) with combinations of factors including i) the presence or absence of the predator, ii) the depth of the shoals in the water column (at the surface, $\leqslant$ 45 mm from the surface, or below the surface, $>$ 45 mm from the surface), and iii) the plane of projection (XY or XZ plane) were run. All factors were treated as categorical variables and a full list of the models can be found in Table 1. We treated depth as a categorical variable because it was clear from diagnostic plots that shoals formed two distinct types of structure (see Figure S4a), and these two types of structures were formed when fish were either above or below 45 mm depth (Figure 1a-d). Trial was included as a random factor in all models as well as the order of that trial within a day (ranging from 1 - 4) as a fixed factor. The corrected Akaike information criterion (AICc) for each model were calculated, as well as the fitted values for each predicted variable. The difference in AICc between the best supported model and each other model in turn was also calculated. Models that were within two AICc units of the best supported model were considered equivalent. The residuals from each model were checked to ensure normality (using QQ plots) and homoscedasticity (using the residuals plotted against the fitted values), and all models were fitted using maximum likelihood.

### *Identifying predators' behavioral states*

From the video footage we established that predators engaged in three key behavioral states: stalking periods (S), strikes (A, attacks), and periods of rest at the bottom of the arena (R, rest). For example, during periods of rest, the predator was often located in the corners of the arena (see Figure S7 for example snapshots and Movie 1). In order to determine the spatial relationship between the predator and prey within these behavioral states, we plotted the distance from the predator to the shoal's centroid as a function of the cosine of the predator's angle to shoal's centroid (Figure 2a). Here, a cosine of -1 or 1 indicates the predator was facing directly away or towards the prey shoal's centroid, respectively. To quantify the transitions between different states of the predator's behavior, we assigned the regions for the distance and direction to a school based on the threshold observation probability ($0.5 \times 10^{-3}$) indicated by the solid lines in Figure 2a. Our method identified exact frames when the states marked in Figure 2a have occurred and these states were validated by comparing against video footage. This allowed us to identify a complete sequence and exact timing of behavioral states in each video. We then constructed a directed behavioral transition graph (Figure 2b), where the sizes of nodes were proportional to a number of state occurrences (i.e., number of video segments capturing a particular behavior of the predator) and the edge widths were proportional to the transitional probabilities (i.e., normalized number of switches between different states). We combined two observed resting phases (R1 and R2; see Figure S3c) as both included times when the predator was inactive.

### *Changes to the shoal's structure surrounding attacks*

To identify when attacks on the group occurred, we manually inspected each video. The nature of the attacks allowed us to identify precisely when an attack was launched. Each attack (Movie 2) involved a period of rapid acceleration (ascending part of the speed curve in Figure 2c), with the predator opening its jaws in an attempt to catch an individual prey, followed by an equivalently fast deceleration (descending part of the speed curve in Figure 2c). We manually defined the time an attack started (t = 0 s) as the frame before the first noticeable change in speed of the predator. Given the temporal resolution of 24 fps, this frame was never ambiguous. To find the time an attack finished, we first computed the 'baseline' speed of the predator in the 0.42 second prior to an attack starting (0.42 s

was chosen to ensure that multiple attacks did not occur within this time period). We then defined the time an attack ended as the intersection between the descending portion of the speed curve and this baseline speed, rounded to the closest frame. This was calculated as 0.46 s (mean ± 0.08 SD) across all attacks. Next, we assessed how quickly the shoal's area changed in both planes in the times surrounding the attacks (i.e. before and after the attack). To do this, we calculated the slope of the change in each projected area (XY or XZ plane) during the three seconds before and, separately, after an attack (see Figure S9). We again used a model comparison approach to assess what factors influenced the rate at which the shoal area changed in size. Fixed effects included: i) Time relative to the attack (i.e. Pre/Post Attack), ii) the plane of projection and iii) the number of attacks that had occurred previously on the shoal + 1. A full list of the models can be found in Table 2. Models included the attack number nested within trial as a random term (as most trials contained multiple attacks). All other model checks and assumptions were considered as before.

*Identifying the prey that were targeted during attacks*

We then assessed what factors influenced the likelihood that a prey would be targeted by a predator. The targeted individual was defined as the individual among the prey that the predator lunged towards (i.e. accelerated towards with its mouth open) during an attack. Note the predator could turn during the attack, but by tracking back in time, we could identify where this targeted individual was on the frame before the lunge was initiated. These targeted individuals were never ambiguous. On the frame before the lunge was initiated (t=0, Figure 2), we manually tracked the position of all the prey (using a bespoke script written in MATLAB) and also determined the coordinates of the single prey that was then targeted. Manually tracking the prey was necessary here to ensure that we could identify all individuals in the group, and therefore their relative risk of being attacked within the complete shoal. In total, we counted 124 attacks from the predators towards the prey across all trials. We then calculated the angle and distance from the predator to each prey, the distance from each prey to the group's centroid, each prey's nearest neighbor (NN) distance, and each prey's nearest neighbor degree (see also Figures S11). To determine the nearest neighbor degree (Barrat *et al.* 2004) of each fish in a given frame, we constructed a nearest neighbor graph, where nodes represented individuals linked by edges directed from their respective nearest neighbors (see Figure S13 for an example). We defined the nearest neighbor degree of each individual as a number of edges directed towards it (i.e., number of times this individual is found to be the nearest neighbor for other group members in a current frame). According to this definition, individuals with lower NN degree were more isolated. The lowest possible NN degree of 0, therefore, corresponded to an individual that was not a nearest neighbor for any other conspecific. We then performed a principal component analysis (PCA) on these five variables to test whether fish that were targeted by the predator differed from non-targeted individuals in PCA space. For this analysis, we computed the z-score for all variables by subtracting the mean and dividing by the standard deviation to provide a common scale for comparison. We tested whether the principle components identified contributed significantly to whether a prey would be targeted or not using a model comparison approach. The response variable in all models was whether a fish had been targeted (1) or not (0), and different models included the presence or absence of the two principle components (see Table 3). In the model comparison we also included a null model with no predictive terms. All models included attack number nested within trial as a random factor. We ranked the models and calculated the change in AICc units between each model and the best supported model. This allowed us to test whether each principle component contributed towards the likelihood of a prey being targeted. Models with an AICc of two units less than the null model were considered to have support.

To statistically determine whether each of the five variables contributed separately to the likelihood of a prey being targeted or not, we again used a model comparison approach. The response variable in these models was again whether a fish had been targeted (1) or not (0). Here, we compared five models, where each model included just one explanatory variable, and a null model containing no explanatory variables. This comparison identifies which explanatory variables were significantly correlated with predation risk, again by identifying those models that performed better ($\Delta$ AICc $>$ 2) than the null model.

Because many empirical and modelling studies on predator-prey interactions only consider information about the locations of predators and prey in a single plane, we wanted to ask whether a 3D approach was necessary to identify which prey were likely to be targeted in the group. To do this, we calculated the five variables described above, but here only used information about the prey and predator's position and orientation in either the XY or XZ plane. We then performed our model comparison approach separately on these XY or XZ scores to see if the model comparisons gave different results to when models used information from both planes (full XYZ dataset). Like above, we also performed our PCA and model comparison on the PC scores for each XY or XZ dataset separately (Figure S12).

## RESULTS

### Spatial distribution and organisation of the prey shoals

Shoals were predominantly observed in two locations in the water column; either towards the surface of the water ($\leqslant$ 45 mm depth) or closer to the bottom of the arena (Figures S3a and S4a). Each of these two locations was associated with a distinct type of shoal structure. When the fish were at the surface of the water, they were spread out in the horizontal (XY) plane, with minimal spread in the vertical (XZ) plane (Figure 1a). In effect, they formed a 'carpet-like', flat structure at the water's surface. When the fish were below the surface of the water, the shoal spread out in both the horizontal and vertical planes, forming more three-dimensional, 'sphere-like' structures (Figure 1b). Evidence for these structures was supported by our model comparison approach, where the best supported models included the interaction term between depth and plane of projection (Table 1; Figure 1). Models that only included these terms as main effects only were not well supported (Table 1). Both shoal structures, 'carpets' and 'spheres', also occurred when the predator was released into the arena (Figure 1c through 1f). However, after introduction of the predator, shoals were primarily observed at the water's surface (see Figure S3b), with the predators spending most of their time at the bottom of the arena (see Figure S3c). A model including whether the predator was present or not and the interaction term between plane and depth was the second best supported model, and within two AIC units of the best supported model. This indicated that predation affected shoal area, with individuals reducing their inter-individual distances in both the vertical and horizontal planes in the presence of the predator (see Figure S5).

Table 1. Models used to assess what factors were important in determining shoal area. The $\Delta$ AICc between the best supported model and subsequent models are shown. Interactions between factors are denoted by an asterisk. All models included the order that a trial was performed on the day of testing as a fixed factor, and individual trial as a random factor. Models within two AIC units of the best supported model were treated as equivalent.

| Explanatory variables | $\Delta$ AICc | d.f |
|---|---|---|
| Plane * Depth | 0 | 7 |
| Plane * Depth + Predator | 0.8 | 8 |
| Plane + Depth | 8.3 | 6 |
| Plane + Depth + Predator | 9.4 | 7 |
| na (null model) | 31.0 | 4 |

### The dynamics of the attacks

While the predators were often observed at the bottom of the arena (see Figure S3c) and often motionless (see Figure S6), the predators also went through periods of stalking the prey, by moving up and into the water column (see Figure S7 and Movie 1). The 'heat' of Figure 2a captures these stalking and resting behavioral states. Periods of rest (R) were characterised by distances $> 0.2$ m between the predator and the shoal's centroid, with the shoal's centroid being almost perpendicular to the predator's direction of travel ($-0.5 < \cos\theta < 0.5$). Here, the resting state, R, appears as two regions (R1 and R2), due to the geometry of the arena creating distinct distances from the shoals centroid at which the predator was likely to be found. The stalking state, S, occurred when the predator remained close to the shoal's centroid (0.075 - 0.14 m) and was oriented directly towards it ($\cos\theta \approx 0.95 - 1.0$). Resting and stalking were the two most frequently observed states (Figure 2b) and most of the behavioral transitions happened between these two states. The stalking periods were 1.65 times more often followed by attacks than the resting periods, as indicated by weights assigned to the corresponding connecting edges. The attack phases, in turn, were 1.64 times more often followed by the periods of rest than by new stalking activities.

Following stalking periods, the predator sometimes attacked the prey (n = 124 events) (Movie 2). We asked whether the prey might be able to predict when an attack was about to be launched based on the movements of the predator leading up to the attack. Before an attack took place, the predator was, on average, moving with a steady low speed of about 0.04 m/s (Figure 2c). The predator's direction of motion before an attack was generally weakly correlated with its direction of travel at the time of a strike (Figure 2d). Nevertheless, there was an increase in the predator's velocity autocorrelation as the time of an attack was approaching, indicative that the predator began targeting a specific part of the shoal, or a specific individual, for as long as 2-3 seconds before the attack. The distance from the predator to the shoal's centroid decreased from the third to the first second before an attack, however, 0.5 s before the strike, this distance increased (Figure 2e), suggesting the prey were expecting an attack and had begun evasive manoeuvres. Even before these evasive manoeuvres, the configuration of a shoal changed (Figure 2f). Both

the horizontal and vertical projected areas decreased in the three seconds before an attack, with the shoal reaching its most compact configuration in the frame before the attack. Overall, the reduction of the shoal's area immediately preceding an attack indicates that individuals were preparing for an attack by moving away from the predator and reducing their inter-individual distances.

80% of the attacks took place at a distance of $< 0.15$ m to prey's centroid (attacks are plotted as black plus signs in Figure 2a), but the attacks were not associated with any specific angle to the shoal's centroid. Predators initiated their attacks when the shoals were not in their usual configurations. Attacks primarily occurred before times when the shoals were larger in the vertical plane than in the horizontal plane (Figure 2f). This was opposite to the configurations that they usually adopted (see Figure 1). The attacks themselves (marked in Figures 2c through 2f by the grey vertical bars) lasted, on average, 0.46 s (mean $\pm$ 0.08 SD). During the initial stage of the attack, the predator simultaneously accelerated (note the speed increase from $\sim 0.04$ to $\sim 0.31$ ms$^{-1}$ in Figure 2c) and adjusted its heading towards the targeted prey (note the velocity de-correlation in Figure 2d). The initial period of the attack was followed by fast deceleration of the predator, comparable in magnitude to its acceleration at the start of the attack (note the two symmetrical slopes of the speed curve in Figure 2c). The predator's speed decreased back to the value before the attack and the velocity of the predator was negatively correlated with its value in the frame immediately before the strike, indicating that the strikes were not always directed at prey directly ahead of the predator, with the predator turning during attacks. The time between attacks was non-random, and many attacks occurred in the seconds following the attack, depicted by the self-loop in Figure 2b (see Figure S8 for the full distribution of times between attacks). In particular, 12% of attacks occurred within six seconds of one another. The total number of attack windows including repetitive and single attacks was 110 for 960 mins of footage.

Prey responded to attacks by moving away from the predator (Figure 2e), which resulted in a 'flash expansion', with the area of the shoal increasing in both the horizontal and vertical planes (Figure 2f). However, before and after this attack, the shoals' area was generally decreasing in both planes. Using the model comparison approach, we asked what factors influenced the rate at which shoal area changed in these times leading up to and following attacks. The most supported model indicated that two factors were most important in determining changes to shoal area (Table 2). First, the time Pre/Post attack was included in the best supported model, indicating that shoals reduced area more quickly in the time following the attacks than in the time leading up to the attack. Second, plane of projection was included in the best supported model, indicating that shoal area changed more rapidly in the XZ plane than in the ZY plane (Figure 2f). This was likely because fish were moving towards the surface of the water, reducing their distance apart more rapidly in the vertical than horizontal plane. There was little evidence that the number of attacks that had previously occurred on the shoal affected these responses (Table 2).

Table 2. Models used to assess what factors were important in determining how the shoal area changed in the times leading up to and following an attack. Interactions between factors are denoted by an asterisk. All models included the order that a trial was performed on the day of testing as a fixed factor, and attack nested within trial as a random factor. The $\Delta$ AICc between the best supported model and subsequent models are shown.

| Explanatory variable | $\Delta$ AICc | d.f |
|---|---|---|
| Pre/Post Attack + Plane | 0 | 7 |
| Pre/Post Attack + Attack Number | 5.2 | 7 |
| na (null model) | 10.9 | 5 |
| Pre/Post Attack + Plane + Attack Number | 17.1 | 8 |
| Pre/Post Attack*Plane + Attack Number | 23.4 | 9 |
| Plane + Attack Number | 40.0 | 7 |

### Targeted individuals

While predators were often observed to stalk and attack the shoals, no prey were captured by the predators in any of the trials. Although prey were not captured, we could identify which individuals were targeted during these attacks, and asked whether this targeting was related to the spatial position of those individuals relative to the predator and others in the shoal. To do this, we performed a principal component analysis on five key spatial characteristics of the predator-prey and prey-prey interactions (Figure 3). The first two principal components explained 63% of the variance in our data (Figure S10). Figure 3 shows an almost complete separation of the targeted and non-targeted individuals into two distinct clusters in the PCA-space. Measures capturing prey-prey interactions (i.e. nearest neighbor distances, distance to the centroid of the group, and nearest neighbor degree) loaded predominantly onto PC1 (see vectors in Figure 3). The angle and distance from the predator to each prey, measures capturing predator-prey interactions, loaded predominantly onto PC2. Using our model comparison approach, we asked whether each of

Table 3. The Δ AICc for models assessing which principle components affected the likelihood a prey would be targeted by the predator. In these models, the response variable was whether a fish was targeted (1) or not (0), and we compared whether models including an additional factor were better at predicting whether a fish was targeted compared to a null model including no predictive terms (i.e. if Δ AICc > 2 between the model of interest and the null model). All models fitted this criteria. All models included the attack number nested within trial as a random factor.

| Explanatory variable | Δ AICc | d.f |
|---|---|---|
| PC2 | 0 | 4 |
| PC1 + PC2 | 1.1 | 5 |
| PC1 | 737.0 | 4 |
| na (null model) | 874.9 | 3 |

Table 4. The Δ AICc for models explaining which individual in the group was targeted by the predator relative to the best supported model (distance between predator and prey). In these models, the response variable was whether a fish was targeted (1) or not (0). We compare whether models including an additional factor were better at predicting whether a fish was targeted compared to a null model including no predictive terms (i.e. if Δ AICc > 2 between the model of interest and the null model). All models fit this criteria.

| Explanatory variable | Δ AICc | d.f |
|---|---|---|
| Distance between predator and prey | 0 | 4 |
| Angle between predator heading and prey position | 148.9 | 4 |
| Distance to nearest neighbor | 339.9 | 4 |
| Distance to centre of the group | 408.9 | 4 |
| Node Score | 421.2 | 4 |
| na (null model) | 474.6 | 3 |

these principle components contributed significantly to the likelihood that a prey would be targeted by the predator. While the top supported model only included PC2, the second (and equivalently well-supported model) also included PC1 (Table 3). All models performed significantly better than the null model in determining whether a prey would be targeted or not (Δ AICc > 2). Both PC1 and PC2 terms, therefore, were important in predicting the risk of predation to prey (Table 3).

To test whether each variable in turn contributed significantly to the likelihood a prey would be targeted or not, we used our model comparison approach to see whether models including these single variables outperformed a null model in their predictive power. All models including these single terms performed significantly better than the null model (all Δ AICc between null model and comparison model were > 2) (Table 4). Therefore, all single factors, at least to some degree, influenced the risk of being targeted by the predator. Prey were more likely to be targeted by the predator if the predator was closer to them, and if the predator was facing them (see Figures S11a&b). Prey were also more likely to be targeted when they were further from their nearest neighbor, further from the centre of group, and more isolated (i.e. had a lower nearest neighbor degree) (see Figures S11c through S11e).

We then asked whether the likelihood an individual would be targeted or not could be predicted based on information from only a single (XY or XZ) plane. To do this, we calculated each variable (angle to the predator, distance to the predator, nearest neighbor distance, distance to the centroid of the group, and nearest neighbor degree) using information from only the horizontal or vertical planes separately. In these partitioned data sets, targeted and non-targeted individuals still separated in PCA space (Figure S12). This was particularly apparent in the dataset only using information from the XY, horizontal plane (Figure S12a). Our model comparison approach on the principle components highlighted, like before, that the best supported models contained both PC1 and PC2 scores (Table S1). Similarly, the model comparison approach on the individual measures highlighted that the ordering of models did not change in either the XY or XZ datasets from the ordering of models in the full XYZ dataset (see Table S2). Moreover, all explanatory variables in these partitioned data-sets still contributed significantly to predicting whether a prey was targeted or not (Table S2).

## DISCUSSION

Our results demonstrate that fish shoals adjust their structure and organisation in three-dimensions both in response to the shoal's location in the water column, the presence or absence of predators, and in response to predator attacks. Shoals formed two discrete types of structures depending on their depth. At the surface, shoals formed carpet-like flat structures, and at depth, organised their spatial distribution in both vertical and horizontal planes. Both pre-

and post-attacks, a shoal's area in both horizontal and vertical planes reduced, although this reduction was more pronounced in the vertical XZ plane than in the horizontal XY plane. The discrete nature of attacks allowed us to identify which prey individual was targeted, and we identified that both predatory-prey interactions (distance and angle to prey) and prey-prey interactions (nearest neighbor distance, nearest neighbor degree and distance to the centre of the group) were important in determining whether a prey was targeted by a predator or not.

The organisation of groups in three-dimensions is expected to change under increased risk as individuals attempt to minimise their domains of danger by decreasing their separation distances (Hamilton 1971). Indeed we found experimental evidence to support this prediction, as groups became more compact in both XY and XZ planes following introduction of the predator. It has also been predicted that selfish-herding can result in two types of group structure depending on individuals' location in space, particularly in relation to boundaries in the environment (Vine 1971). Again, we found support for this prediction, where shoals formed flat, carpet-like structures at the water's surface, and more three-dimensional sphere-like geometries at depth. The emergence of these group structures is likely owing to simple behavioural rules governing how individuals respond to their neighbours' movements and positions (Tunstrøm *et al.* 2013). Indeed, self-propelled simulation models using simple attraction, repulsion and alignment rules can produce realistic three-dimensional group structures (Hemelrijk *et al.* 2010). Few of these models, however, have incorporated realistic boundary effects, such as the surface of the water, to investigate what impacts this has for the collective structures that emerge (but see Hemelrijk *et al.* (2010)). The formation of the carpet-like structures, for example, may simply be a product of individuals compressing against the surface as they move away from the threat below, combined with social cohesion. A future direction could be to assess the risk posed to individuals when occupying different types of group structure, and ask when and how individuals decide to switch between these types of structure depending on the costs and benefits those structures provide individuals.

While both planes provided information to identify which prey would be targeted during attacks, partitioning the dataset to assess whether the risk to individuals could be identified solely from data in either the XY (horizontal) or XZ (vertical) plane showed that targeted individuals could still be identified using information from only a single plane. Moreover, metrics based on predator-prey and prey-prey interactions were both important in assessing this risk. Together, these results provide validity for models investigating selfish-herd effects in two-dimensions (Morrell & Romey 2008, Morrell *et al.* 2010, Viscido *et al.* 2001). Such models have often assessed the risk posed to individuals in groups based on their positions relative to predators and other prey in two dimensions only. While this may appear to be an over-simplification, our results demonstrate that such models remain realistic because animal groups indeed form two-dimensional group structures, even in three-dimensional worlds. It also demonstrates that Hamilton's original assumption that a predator could attack from anywhere within a two-dimensional group remains valid (Hamilton 1971), because predators approached groups from below, allowing them the potential to target any individual in the carpet-like two-dimensional structure above.

While predators could attack prey anywhere within the group, especially when the prey were at the group's surface, predators targeted prey closer towards the edge of groups, or more isolated individuals. This effect, known as 'marginal predation', is a well established phenomena (Duffield & Ioannou 2017, Milinski 1977, Romey *et al.* 2007). When approaching groups during stalking periods, however, the predators focussed their attention on the shoal's centroid. This strategy could represent a method used by the predators to break up the shoals in order to isolate individuals (see Movie 2). Indeed, similar strategies are observed in group hunting predators, that form line-formations in order to break apart prey groups (Handegard *et al.* 2012). Predators are thought to isolate individuals as confusion effects make it difficult to target prey in dense moving groups (Ioannou *et al.* 2007, Landeau & Terborgh 1986, Ruxton *et al.* 2007). The observation that 12% attacks occurred within six seconds of one another could suggest that predators might use periods when shoals are reorganising to target individuals that have become separated from others in previous attacks. Such a tactic may increase predator success rates, although in this study, predators were never successful in their attacks. An interesting future area of research could be to investigate how group structure and space use changes when groups are under attack from predators with different hunting strategies, for example, in response to an aerial or group hunting predators. There is some evidence that golden shiners *Notemigonus crysoleucas* move away from the water's surface and also increase the depth of their schools following aerial strikes, and schools of fish can move differently in the horizontal or vertical plane according to whether birds or dolphins are attacking them (Vaughn *et al.* 2010). Investigating different predatory tactics in both empirical work and simulations will shed new insights into how and why predators target the individuals they select in groups (Nishimura 2002), and how prey adopt different behavioral strategies to overcome different predatory tactics (Herbert-Read *et al.* 2017).

It is important to discuss whether the predator-prey interactions recorded in the laboratory would also be observed in nature, and to ask what factors could have influenced the expression of particular behaviours. While the shoals in our experiment were constrained to an aquarium, wild shoals of fish have been observed to form both two-dimensional structures at the water's surface (Ward *et al.* 2017) and more three-dimensional structures in pelagic environments (Gerlotto *et al.* 1994, Paramo *et al.* 2010). In the experiments conducted here, the structures adopted by the group did not occupy the entire horizontal or vertical space of the arena (see Fig. S5a&b), hence crowding effects are unlikely to

have contributed strongly towards the adoption of particular shoal structures. Another conspicuous difference between the arena and more natural environments where *P. signifer* and *P. grandiceps* inhabit, was the absence of vegetation or cover in the experiment. Previous experiments on flathead minnows (*Pimephales promelas*) have demonstrated that fish increase their tendency to shoal in the absence of cover (Savino & Stein 1989), hence our experimental set-up may have induced particularly high degrees of shoaling. The presence or absence of structural complexity in aquatic environments can also induce specific types of hunting behaviour in predators. Lined seahorses (*Hippocampus erectus*), for example, switch from 'sit and wait' tactics to pursuit tactics when structure in the environment is removed (James & Heck Jr 1994). Future experiments, therefore, should investigate the shoal structures adopted by prey groups, as well as predator tactics, in environments where habitat complexity is manipulated. We should also question whether the attack rates of *P. grandiceps* represent those that would be observed in nature. While the attack rates in the experiment were low (124 attacks in 960 minutes, equating to 7.75 attacks per hour), these rates are comparable to attack rates of pike (*Esox lucius*) and largemouth bass (*Micropterus salmoides*) preying on bluegills (*Lepomis macrochirus*) and fathead minnows (*P. promelas*) in more naturalistic experimental conditions ($< \sim 10$ per hour) (Savino & Stein 1989). The noticeable absence of any successful attacks may be attributed to predators being highly conspicuous against the light background of the arena. Considering camouflage is a well-used predatory strategy (Merilaita *et al.* 2017), conspicuousness of the predator may have given prey ample opportunity to avoid the predator, and hence ultimately reduce capture success rates. With the advent of high-resolution sonar and comparable methods in the field (Handegard *et al.* 2012) detailed observations of predator-prey interactions can now be recorded to assess natural capture success rates in the wild (Herbert-Read *et al.* 2016). This will provide valuable ground-truths for predator-prey interactions. Nevertheless, experiments where environmental conditions can be tightly controlled and manipulated offer significant opportunity to experimentally test the factors shaping the structure and dynamics of predator-prey interactions.

## Ethics statement

Investigations were performed under ethical permission from the University of Sydney's Ethics Committee (ref. number: L04/6- 2009/3/5083).

## Acknowledgements

We thank N. Kolm and three anonymous referees for helpful comments on an earlier version of the manuscript.

## Competing interests

The authors declare no competing or financial interests.

## Author contributions

Conceptualization: J.E.H.-R., M.R., A.J.W.W., D.J.T.S.; Methodology: M.R., J.E.H.-R; Analysis: M.R., J.E.H.-R., A.S. C.C.I; Writing: J.E.H.-R., M.R., A.S., D.J.T.S., A.J.W.W., C.C.I.

## Funding

This work is supported by a Knut and Alice Wallenberg Foundation grant no. 2013.0072 to D.J.T.S, and a Swedish Research Council Grant, 2018– 04076, awarded to J.E.H-R.

## Data availability

Analyses reported in this article can be reproduced using the data provided by Romenskyy et al. (2019).

**Supplementary information**

Supplementary information is available online

---


Abrahams, M.V. & Colgan, P.W. (1985) Risk of predation, hydrodynamic efficiency and their influence on school structure. *Environ. Biol. Fish.* **13**, 195–202.

Attanasi, A., Cavagna, A., Del Castello, L., Giardina, I., Melillo, S., Parisi, L., Pohl, O., Rossaro, B., Shen, E., Silvestri, E. *et al.* (2014) Collective behaviour without collective order in wild swarms of midges. *PLoS Comput. Biol.* **10**, e1003697.

Axelsen, B.E., Anker-Nilssen, T., Fossum, P., Kvamme, C. & Nøttestad, L. (2001) Pretty patterns but a simple strategy: predator-prey interactions between juvenile herring and atlantic puffins observed with multibeam sonar. *Can. J. Zoolog.* **79**, 1586–1596.

Ballerini, M., Cabibbo, N., Candelier, R., Cavagna, A., Cisbani, E., Giardina, I., Lecomte, V., Orlandi, A., Parisi, G., Procaccini, A. *et al.* (2008) Interaction ruling animal collective behavior depends on topological rather than metric distance: Evidence from a field study. *Proc. Nat. Acad. Sci.* **105**, 1232–1237.

Barrat, A., Barthélemy, M., Pastor-Satorras, R. & Vespignani, A. (2004) The architecture of complex weighted networks. *Proc. Nat. Acad. Sci.* **101**, 3747–3752.

Becker, A. & Laurenson, L.J. (2008) Seasonal and diel comparisons of the diets of four dominant fish species within the main channel and flood-zone of a small intermittently open estuary in south-eastern australia. *Mar. Freshwater Res.* **58**, 1086–1095.

Benoit-Bird, K.J. & Au, W.W. (2009) Cooperative prey herding by the pelagic dolphin, stenella longirostris. *J. Acoust. Soc. Am.* **125**, 125–137.

Branson, K., Robie, A.A., Bender, J., Perona, P. & Dickinson, M.H. (2009) High-throughput ethomics in large groups of drosophila. *Nat. Methods* **6**, 451–457.

Brierley, A.S. & Cox, M.J. (2010) Shapes of krill swarms and fish schools emerge as aggregation members avoid predators and access oxygen. *Curr. Biol.* **20**, 1758–1762.

Carere, C., Montanino, S., Moreschini, F., Zoratto, F., Chiarotti, F., Santucci, D. & Alleva, E. (2009) Aerial flocking patterns of wintering starlings, sturnus vulgaris, under different predation risk. *Anim. Behav.* **77**, 101–107.

Chen, Y. & Kolokolnikov, T. (2014) A minimal model of predator–swarm interactions. *J. Roy. Soc. Inter.* **11**, 20131208.

Chrásková, J., Kaminsky, Y. & Krekule, I. (1999) An automatic 3d tracking system with a pc and a single tv camera. *J. Neurosci. Meth.* **88**, 195 – 200.

Couzin, I.D., Krause, J., James, R., Ruxton, G.D. & Franks, N.R. (2002) Collective memory and spatial sorting in animal groups. *J. Theor. Biol.* **218**, 1–11.

De Vos, A. & O'Riain, M.J. (2010) Sharks shape the geometry of a selfish seal herd: experimental evidence from seal decoys. *Biol. Lett.* **6**, 48–50.

Duffield, C. & Ioannou, C.C. (2017) Marginal predation: do encounter or confusion effects explain the targeting of prey group edges? *Behav. Ecol.* **28**, 1283–1292.

Gerlotto, F., Freon, P., Soria, M., Cottais, P. & Ronzier, L. (1994) Exhaustive observation of 3d school structure using multibeam side scan sonar: potential use for school classification, biomass estimation and behaviour studies. *ICES CM* **19948**, 26.

Gerlotto, F. & Paramo, J. (2003) The three-dimensional morphology and internal structure of clupeid schools as observed using vertical scanning multibeam sonar. *Aquat. Living Resour.* **16**, 113–122.

Guillard, J., Fernandes, P., Laloë, T. & Brehmer, P. (2011) Three-dimensional internal spatial structure of young-of-the-year pelagic freshwater fish provides evidence for the identification of fish school species. *Limnol. Oceanogr.: Methods* **9**, 322–328.

Hamilton, W.D. (1971) Geometry for the selfish herd. *J. Theor. Biol.* **31**, 295–311.

Handegard, N.O., Boswell, K.M., Ioannou, C.C., Leblanc, S.P., Tjøstheim, D.B. & Couzin, I.D. (2012) The dynamics of coordinated group hunting and collective information transfer among schooling prey. *Curr. Biol.* **22**, 1213–1217.

Handegard, N.O., Holmin, A.J. & Rieucau, G. (2017) Method to observe large scale behavioural waves propagating through fish schools using 4d sonar. *ICES J. Mar. Sci.* **74**, 804–812.

Handegard, N.O. & Williams, K. (2008) Automated tracking of fish in trawls using the didson (dual frequency identification sonar). *ICES J. Mar. Sci.* **65**, 636–644.

Hartley, R. & Zisserman, A. (2003) *Multiple View Geometry in Computer Vision.* Cambridge University Press.

Hemelrijk, C.K. & Hildenbrandt, H. (2012) Schools of fish and flocks of birds: their shape and internal structure by self-organization. *Inter. Foc.* p. rsfs20120025.

Hemelrijk, C.K., Hildenbrandt, H., Reinders, J. & Stamhuis, E.J. (2010) Emergence of oblong school shape: models and empirical data of fish. *Ethol.* **116**, 1099–1112.

Herbert-Read, J.E. (2016) Understanding how animal groups achieve coordinated movement. *J. Exp. Biol.* **219**, 2971–2983.

Herbert-Read, J.E., Romanczuk, P., Krause, S., Strömbom, D., Couillaud, P., Domenici, P., Kurvers, R.H., Marras, S., Steffensen, J.F., Wilson, A.D. *et al.* (2016) Proto-cooperation: group hunting sailfish improve hunting success by alternating attacks on grouping prey. *Proc. Roy. Soc. B. Bio. Sci.* **283**, 20161671.

Herbert-Read, J.E., Ward, A.J., Sumpter, D.J. & Mann, R.P. (2017) Escape path complexity and its context dependency in pacific blue-eyes (pseudomugil signifer). *J. Exp. Biol.* **220**, 2076–2081.

Hirsch, B.T. & Morrell, L.J. (2011) Measuring marginal predation in animal groups. *Behav. Ecol.* **22**, 648–656.
Ioannou, C., Guttal, V. & Couzin, I. (2012) Predatory fish select for coordinated collective motion in virtual prey. *Science* **337**, 1212–1215.
Ioannou, C., Tosh, C., Neville, L. & Krause, J. (2007) The confusion effect—from neural networks to reduced predation risk. *Behav. Ecol.* **19**, 126–130.
Ioannou, C.C., Couzin, I.D., James, R., Croft, D.P. & Krause, J. (2011) Social organisation and information transfer in schooling fish. *Fish cognition and behavior* **2**, 217–239.
Ioannou, C.C., Rocque, F., Herbert-Read, J.E., Duffield, C. & Firth, J.A. (2019) Predators attacking virtual prey reveal the costs and benefits of leadership. *Proceedings of the National Academy of Sciences* **116**, 8925–8930.
James, P.L. & Heck Jr, K.L. (1994) The effects of habitat complexity and light intensity on ambush predation within a simulated seagrass habitat. *J. Exp. Mar. Biol. Ecol.* **176**, 187–200.
James, R., Bennett, P. & Krause, J. (2004) Geometry for mutualistic and selfish herds: the limited domain of danger. *J. Theor. Biol.* **228**, 107–113.
Johnsen, E., Rieucau, G., Ona, E. & Skaret, G. (2017) Collective structures anchor massive schools of lesser sandeel to the seabed, increasing vulnerability to fishery. *Mar. Ecol. Prog. Ser.* **573**, 229–236.
Krause, J. (1994) Differential fitness returns in relation to spatial position in groups. *Biol. Rev.* **69**, 187–206.
Krause, J., Herbert-Read, J.E., Seebacher, F., Domenici, P., Wilson, A.D., Marras, S., Svendsen, M.B.S., Strömbom, D., Steffensen, J.F., Krause, S. *et al.* (2017) Injury-mediated decrease in locomotor performance increases predation risk in schooling fish. *Phil. Trans. R. Soc. B* **372**, 20160232.
Landeau, L. & Terborgh, J. (1986) Oddity and the 'confusion effect' in predation. *Anim. Behav.* **34**, 1372–1380.
Magurran, A.E. & Pitcher, T.J. (1987) Provenance, shoal size and the sociobiology of predator-evasion behaviour in minnow shoals. *Proc. Roy. Soc. B. Bio. Sci.* **229**, 439–465.
Major, P.F. & Dill, L.M. (1978) The three-dimensional structure of airborne bird flocks. *Behav. Ecol. Sociobiol.* **4**, 111–122.
Merilaita, S., Scott-Samuel, N.E. & Cuthill, I.C. (2017) How camouflage works. *Phil. Trans. Roy. Soc. B: Biol. Sci.* **372**, 20160341.
Milinski, M. (1977) Experiments on the selection by predators against spatial oddity of their prey. *Ethol.* **43**, 311–325.
Morrell, L.J. & Romey, W.L. (2008) Optimal individual positions within animal groups. *Behav. Ecol.* **19**, 909–919.
Morrell, L.J., Ruxton, G.D. & James, R. (2010) Spatial positioning in the selfish herd. *Behav. Ecol.* **22**, 16–22.
Morrell, L.J., Ruxton, G.D. & James, R. (2011) The temporal selfish herd: predation risk while aggregations form. *Proc. Roy. Soc. B. Bio. Sci.* **278**, 605–612.
Nishimura, S.I. (2002) A predator's selection of an individual prey from a group. *Biosystems* **65**, 25–35.
Nøttestad, L., Fernö, A., Mackinson, S., Pitcher, T. & Misund, O.A. (2002) How whales influence herring school dynamics in a cold-front area of the norwegian sea. *ICES J. Mar. Sci.* **59**, 393–400.
O'Brien, D. (1989) Analysis of the internal arrangement of individuals within crustacean aggregations (euphausiacea, mysidacea). *J. Exp. Mar. Biol. Ecol.* **128**, 1–30.
Paramo, J., Gerlotto, F. & Oyarzun, C. (2010) Three dimensional structure and morphology of pelagic fish schools. *J. Appl. Ichthyol.* **26**, 853–860.
Parrish, J.K. & Hamner, W.M. (1997) *Animal groups in three dimensions: how species aggregate.* Cambridge University Press.
Partridge, B.L., Pitcher, T., Cullen, J.M. & Wilson, J. (1980) The three-dimensional structure of fish schools. *Behav. Ecol. Sociobiol.* **6**, 277–288.
Pitcher, T.J. & Wyche, C.J. (1983) Predator avoidance behaviour of sand-eel schools: why schools seldom split. *Predators and prey in fishes* **54**, 193–204.
Procaccini, A., Orlandi, A., Cavagna, A., Giardina, I., Zoratto, F., Santucci, D., Chiarotti, F., Hemelrijk, C.K., Alleva, E., Parisi, G. *et al.* (2011) Propagating waves in starling, sturnus vulgaris, flocks under predation. *Anim. Behav.* **82**, 759–765.
Pusey, B., Kennard, M. & Arthington, A. (2004) *Freshwater fishes of north-eastern Australia.* CSIRO publishing.
Rieucau, G., Boswell, K.M., De Robertis, A., Macaulay, G.J. & Handegard, N.O. (2014) Experimental evidence of threat-sensitive collective avoidance responses in a large wild-caught herring school. *PLoS One* **9**, e86726.
Rieucau, G., Holmin, A.J., Castillo, J.C., Couzin, I.D. & Handegard, N.O. (2016) School level structural and dynamic adjustments to risk promote information transfer and collective evasion in herring. *Anim. Behav.* **117**, 69–78.
Romey, W., Walston, A. & Watt, P. (2007) Do 3-d predators attack the margins of 2-d selfish herds? *Behav. Ecol.* **19**, 74–78.
Ruxton, G.D., Jackson, A.L. & Tosh, C.R. (2007) Confusion of predators does not rely on specialist coordinated behavior. *Behav. Ecol.* **18**, 590–596.
Savino, J.F. & Stein, R.A. (1989) Behavioural interactions between fish predators and their prey: effects of plant density. *Anim. Behav.* **37**, 311–321.
Seghers, B.H. (1974) Schooling behavior in the guppy (poecilia reticulata): an evolutionary response to predation. *Evolution* pp. 486–489.
Tunstrøm, K., Katz, Y., Ioannou, C.C., Huepe, C., Lutz, M.J. & Couzin, I.D. (2013) Collective states, multistability and transitional behavior in schooling fish. *PLoS Comput. Biol.* **9**, e1002915.
Vaughn, R., Würsig, B. & Packard, J. (2010) Dolphin prey herding: prey ball mobility relative to dolphin group and prey ball sizes, multispecies associates, and feeding duration. *Mar. Mammal Sci.* **26**, 213–225.
Vine, I. (1971) Risk of visual detection and pursuit by a predator and the selective advantage of flocking behaviour. *J. Theor. Biol.* **30**, 405–422.
Viscido, S.V., Miller, M. & Wethey, D.S. (2001) The response of a selfish herd to an attack from outside the group perimeter. *J. Theor. Biol.* **208**, 315–328.

Viscido, S.V., Parrish, J.K. & Grünbaum, D. (2004) Individual behavior and emergent properties of fish schools: a comparison of observation and theory. *Mar. Ecol. Prog. Ser.* **273**, 239–250.
Ward, A. & Webster, M. (2016) Sociality. *Sociality: The Behaviour of Group-Living Animals*, pp. 1–8, Springer.
Ward, A.J., Schaerf, T.M., Herbert-Read, J.E., Morrell, L., Sumpter, D.J. & Webster, M.M. (2017) Local interactions and global properties of wild, free-ranging stickleback shoals. *R. Soc. Open Sci.* **4**, 170043.
Watts, I., Nagy, M., Holbrook, R.I., Biro, D. & Burt de Perera, T. (2017) Validating two-dimensional leadership models on three-dimensionally structured fish schools. *R. Soc. Open Sci.* **4**.
Yang, W.C. & Schmickl, T. (2019) Collective motion as an ultimate effect in crowded selfish herds. *Sci. Rep.* **9**, 6618.

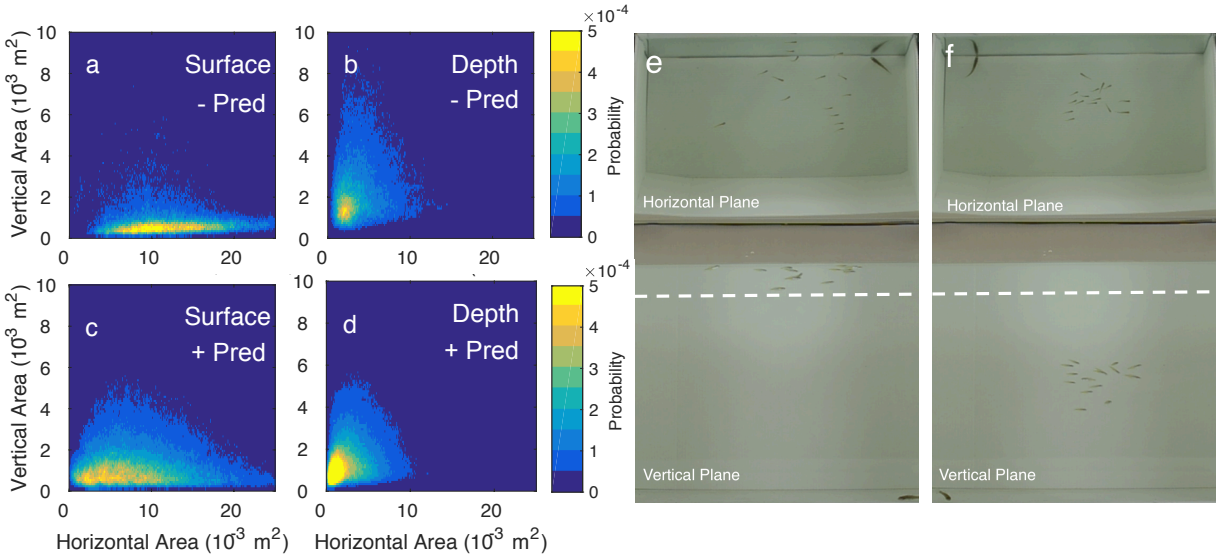


Figure 1. **Shoal spatial statistics.** Shoals form two types of structure: carpet-like flat structures at the waters' surface ($\leqslant$ 45 mm from the surface of the water) (a, c and e) and sphere-like structures at depth ($>$ 45 mm from the surface of the water) (b, d and f). The axes' labels, 'vertical' and 'horizontal' areas correspond to the area that the shoal occupied in the vertical and horizontal planes respectively. Notice that the vertical area is generally less than the horizontal area in (a) and (c), indicative that the shoals were compressed in the vertical plane, forming 'carpets' at the water's surface. Notice that the vertical and horizontal areas in (b) and (d) are generally proportional to one another, indicative that the shoals were forming 'spheres' at depth. (a) and (b) show times without the predator, and (c) and (d) show times with the predator. Notice that in (c) versus (a) and (d) versus (b), the heat moves towards the lower left corner of the plot, indicative that the shoal's area in both planes reduced following introduction of the predator. See Figure S4 for plots where structures have not been separated according to depth. The heat in the plots represents the likelihood of the shoals being observed in each location of the parameter space. Panels (e) and (f) show frames from one of the trials when the shoal was in a carpet (e) or sphere-like (f) structure. The horizontal dashed line represents a water depth of 45 mm.

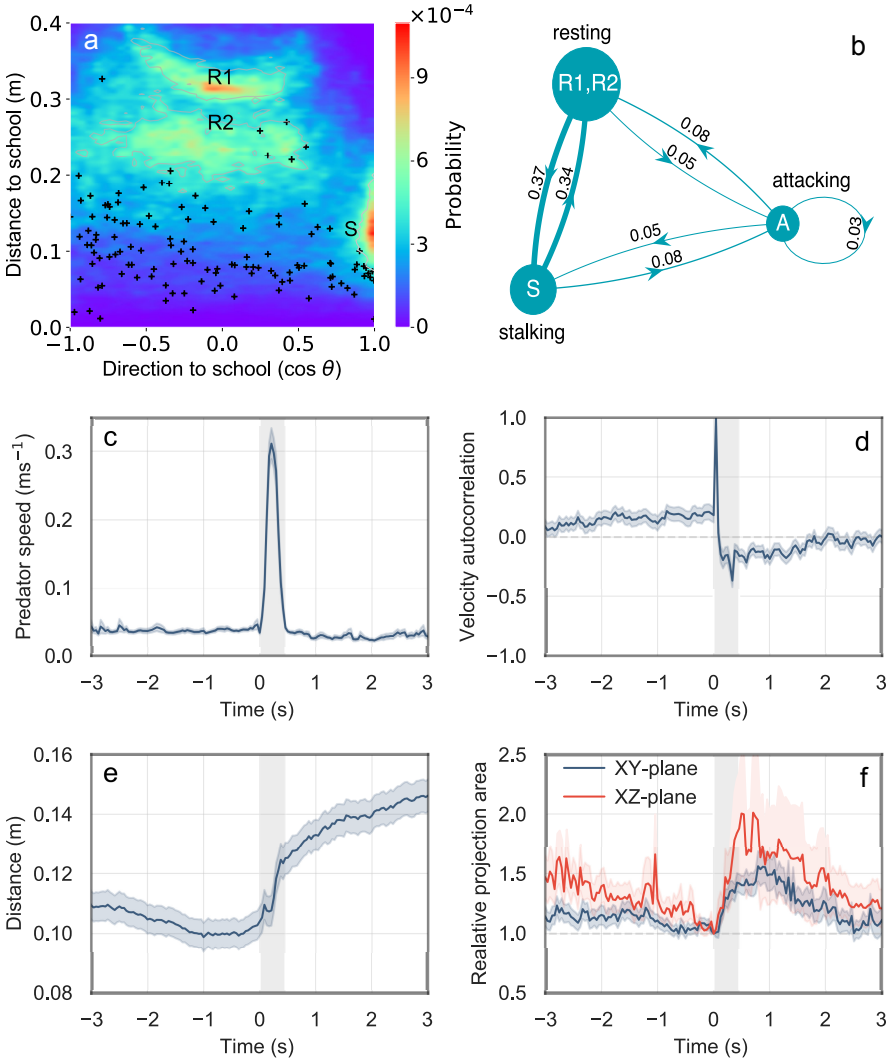


Figure 2. **Behavioral states of the predator-prey dynamics, motion statistics and behavioral progression of the attacks.** (a) Likelihood of the position and orientation of the predator relative to the shoal's centroid. The relative position is represented as: (horizontal axis) the cosine of the angle $\theta$ between the predator's orientation and the centroid of the group; and (vertical axis) the predator's distance to the centroid. The color bar shows the likelihood of each combination of $\cos\theta$ and distance. The three distinct behavioral states of the predator are: resting (R1 and R2), stalking (S) and attacking (A). All attacks are plotted over the color map as black plus signs. (b) Behavioral transition graph. Sizes of the nodes are proportional to the state probabilities (the logarithmic scale is applied for visual clarity). Widths of the edges are proportional to the transition probabilities indicated next to them.

In this figure, repetitive attacks were classified as attacks that occurred within 6 seconds of one another, but see Figure S8 for the full distribution of times between attacks. (c) Average speed of the predator before, during and after the attack. (d) Autocorrelation function of the predator velocity, $C(t) = \langle \mathbf{V}(0) \cdot \mathbf{V}(t) \rangle$, where $t$ denotes time from the beginning of the attack and $\langle\rangle$ stands for an average over all attacks. The autocorrelation is computed for every video frame from -3 to 3 s with respect to the attack time. The dotted line aids visual assessment of the sign of correlation. (e) Distance from the predator to shoal's centroid. (f) Average relative shoal projected area in the XY and XZ plane. The dotted line provides a comparison with the values of relative projected areas at t = 0. The grey bar around $t = 0 - 0.46$ s in plots c-f denotes the attack. The shaded areas around each data curve represent the standard errors. Averages are taken over all 124 attacks. t = 0 was determined as the frame before the predator was observed to rapidly accelerate towards a prey.

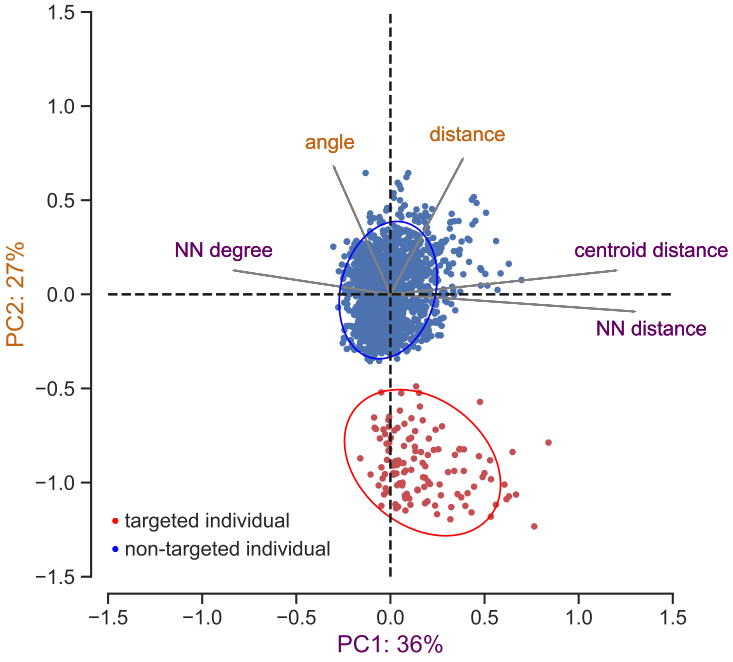


Figure 3. **Principal component analysis of prey spatial statistics prior to each attack ($t = 0$).** The ellipses denote the 95% confidence limits. The percentages in the axis labels indicate the amount of variance explained by the corresponding components. The arrows are pointing in the direction of the variables, as projected into PC1-PC2 plane. Targeted fish are shown as red points, non-targeted fish are shown as blue points. PC1 (maroon) captures more of the prey-prey interactions (NN distance = nearest neighbor distance, centroid distance = distance of individual from the group centroid, NN degree = nearest neighbor degree), with targeted fish being more isolated from other group members. PC2 (orange), on the other hand, captures the predator-prey interactions, with targeted prey being closer (distance) and more directly in-front (angle) of the predator. See Figure S12 for this analysis performed using information only in the single horizontal or vertical planes.